Electronic Supplementary Material (ESI) for Physical Chemistry Chemical Physics.

Supporting Information

Charge Driven Lateral Structural Evolution of Ions in Electric Double Layer Capacitor Strongly Correlates with Differential Capacitance

Jiale Ma,[ab] Qiangqiang Meng[a] and Jun Fan*[ab]

[a] Department of Materials Science and Engineering, City University of Hong Kong, Hong Kong

[b] City University of Hong Kong Shenzhen Research Institute, Shenzhen 518057, China

1. Simulation process

In this work, before the equilibrium and production run, a pure IL system without graphite has been performed to obtain the density of IL. The equilibrated mass density of pure IL system is 1.27 g/cm^3, which is very close to 1.28 g/cm^3 in original work of the current force field.[1,2] Based on this mass density, 396 ion pairs were randomly placed between two electrodes to generate the initial configuration by PACKMOL package.[3] In the equilibrium part, the initial configuration was first heated from 1 K to 1000 K in 1 ns and equilibrated for 4 ns at 1000 K. Then the system was gradually quenched to 300 K in 7 ns. The equilibration run at 300 K is 10 ns. Based on this result, partial charge was assigned to each C atom on the surface graphite layer and the system was equilibrated for another 11 ns. At last, A 30 ns production run was performed to calculate the EDL properties.

2. Supplementary figures

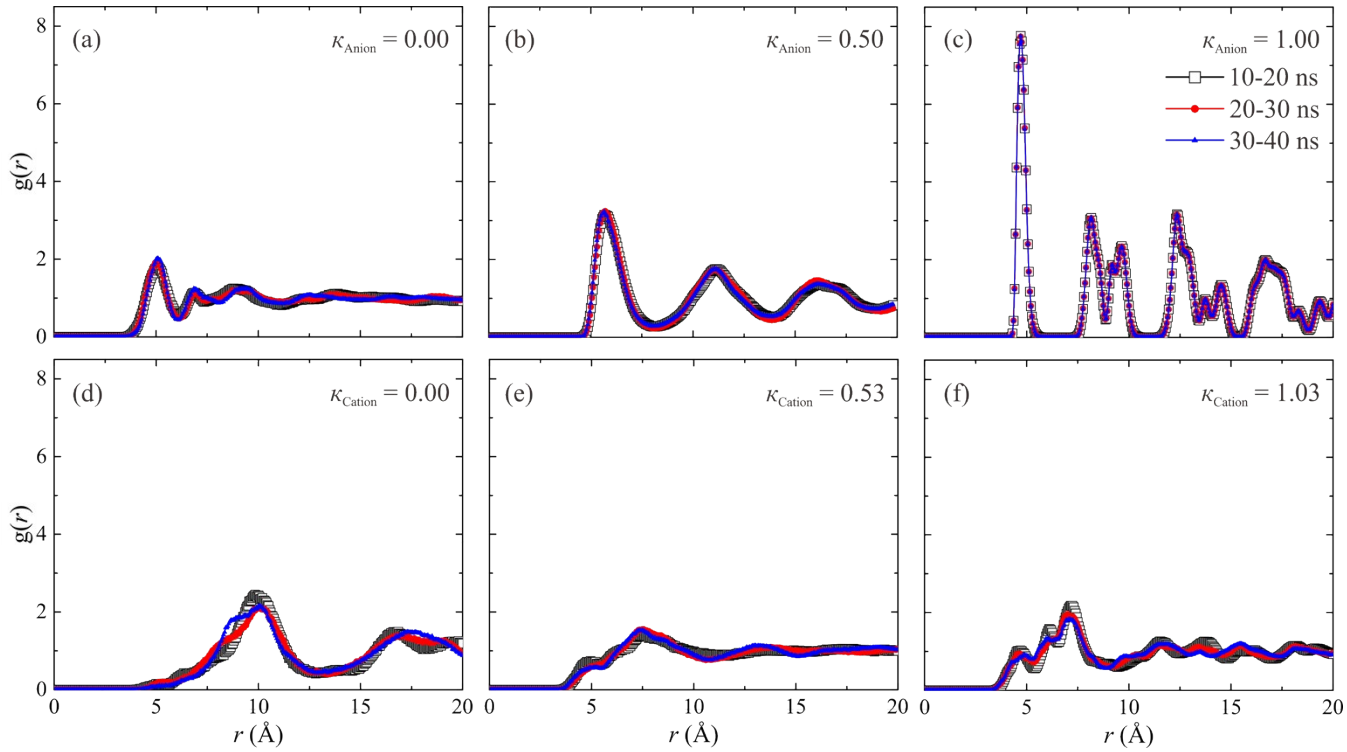

Figure S1 g(r) of ions in different simulation periods. g(r) of PF_6^- and $BMIM^+$ near the electrode are plotted in (a)-(c) and (d)-(f), respectively. The profiles g(r) at 10-20, 20-30 and 30-40 ns are colored in black, red and blue, respectively. κ_{Anion} of (a)-(c) are 0.00, 0.50 and 1.00, while κ_{Cation} of (d)-(f) are 0.00, 0.53 and 1.03, respectively.

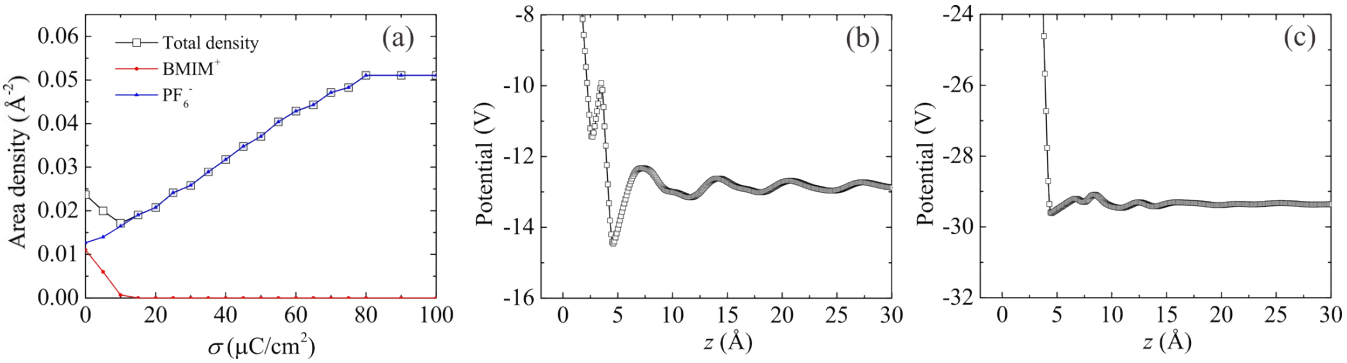

Figure S2 Determination of maximum charge density θ_{max}. The area density of ions in the first layer as a function of surface charge density σ is shown in (a). Two potential profiles across the simulation box in z direction are shown in (b) and (c). The σ values of electrode in (b) and (c) are 40 and 80 μC/cm^2, respectively. The surface layer of electrode locates at z = 0 Å.

With the increasing of surface charge density σ, the ion density of PF_6^- in the first layer first increases linearly and then get saturated at around 80 μC/cm^2. Therefore, the maximum charge density θ_{max} in this work is around 80 μC/cm^2.Then, the potential drop profile at $\sigma = \theta_{max}$ and $\sigma = 1/2\ \theta_{max}$ was shown in (b) and (c). Similar to the ref. 4 and 5, the fluctuated profile indicated the multilayer structure of electric double layer at 40 μC/cm^2, while the flat curve indicate the monolayer structure of electric double layer at 80 μC/cm^2. The θ_{max} = 80 μC/cm^2 of PF_6^- in this work is larger than 50 μC/cm^2, which is the θ_{max} of LJ particle model of PF_6^- in ref. 5. The θ_{max} of all-atom model is much larger than that of LJ particle model, which means more ions can be stored in one monolayer if all atom model was used. The difference of θ_{max} of PF_6^- between LJ particle and all-atom model is consistent with that of BF_4^-. The θ_{max} of BF_4^- LJ particle is about 60 μC/cm^2 [5], while the value of all atom model is 100 μC/cm^2 [6].

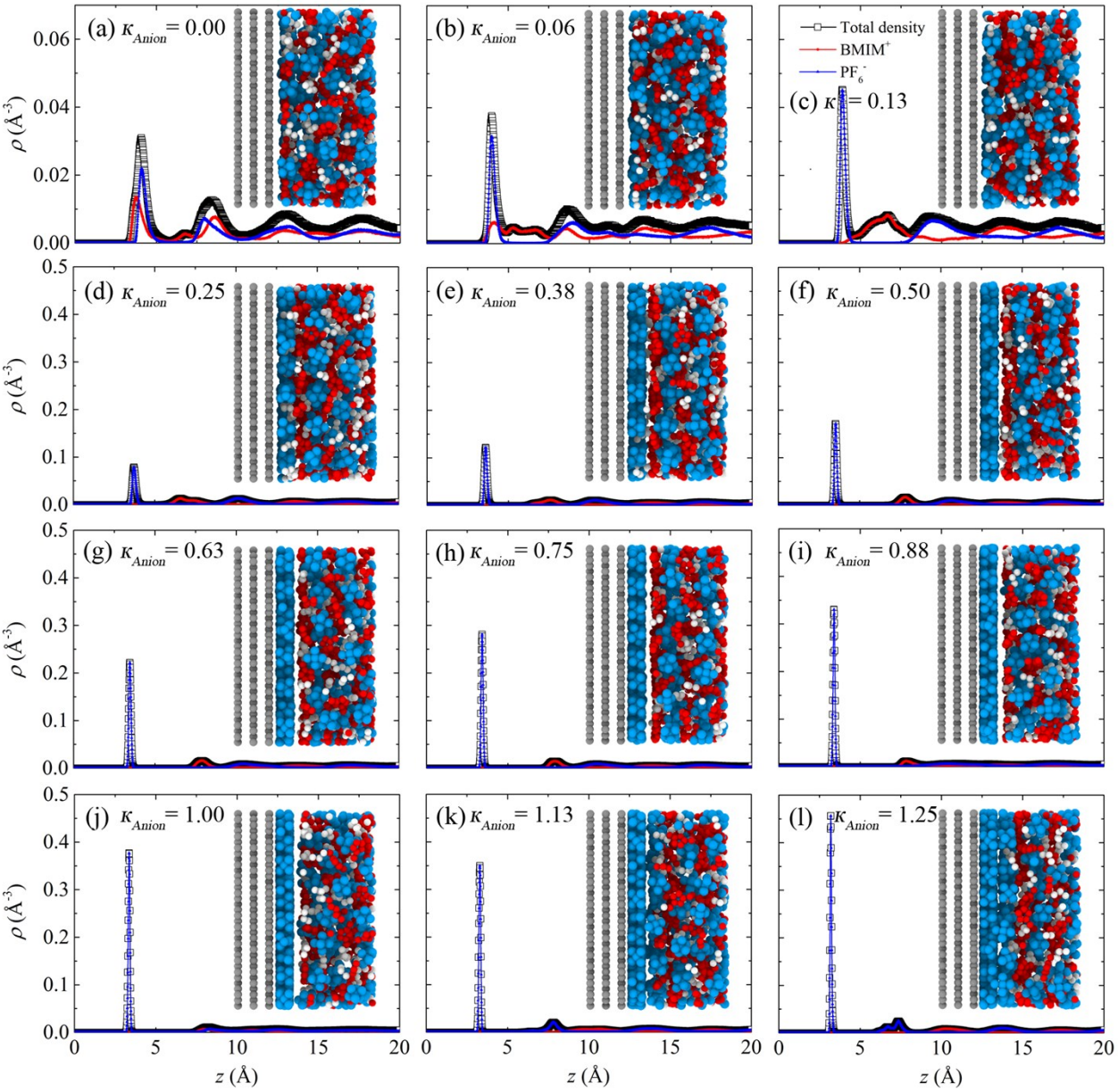

Figure S3. Number density distribution of ions in z direction near anode. The surface charge compensation parameter κ_{Anion} in (a)-(l) is 0.00, 0.06, 0.13, 0.25, 0.38, 0.50, 0.63, 0.75, 0.88, 1.00, 1.13 and 1.25, respectively. The density profiles of $BMIM^+$, PF_6^- and the summation of both ions were colored in red, blue and black, respectively. The coordinates of ions were determined by their center of mass. The surface of the anode is located at $z = 0$. The side views of ions near the anode are shown in the inserted figures.

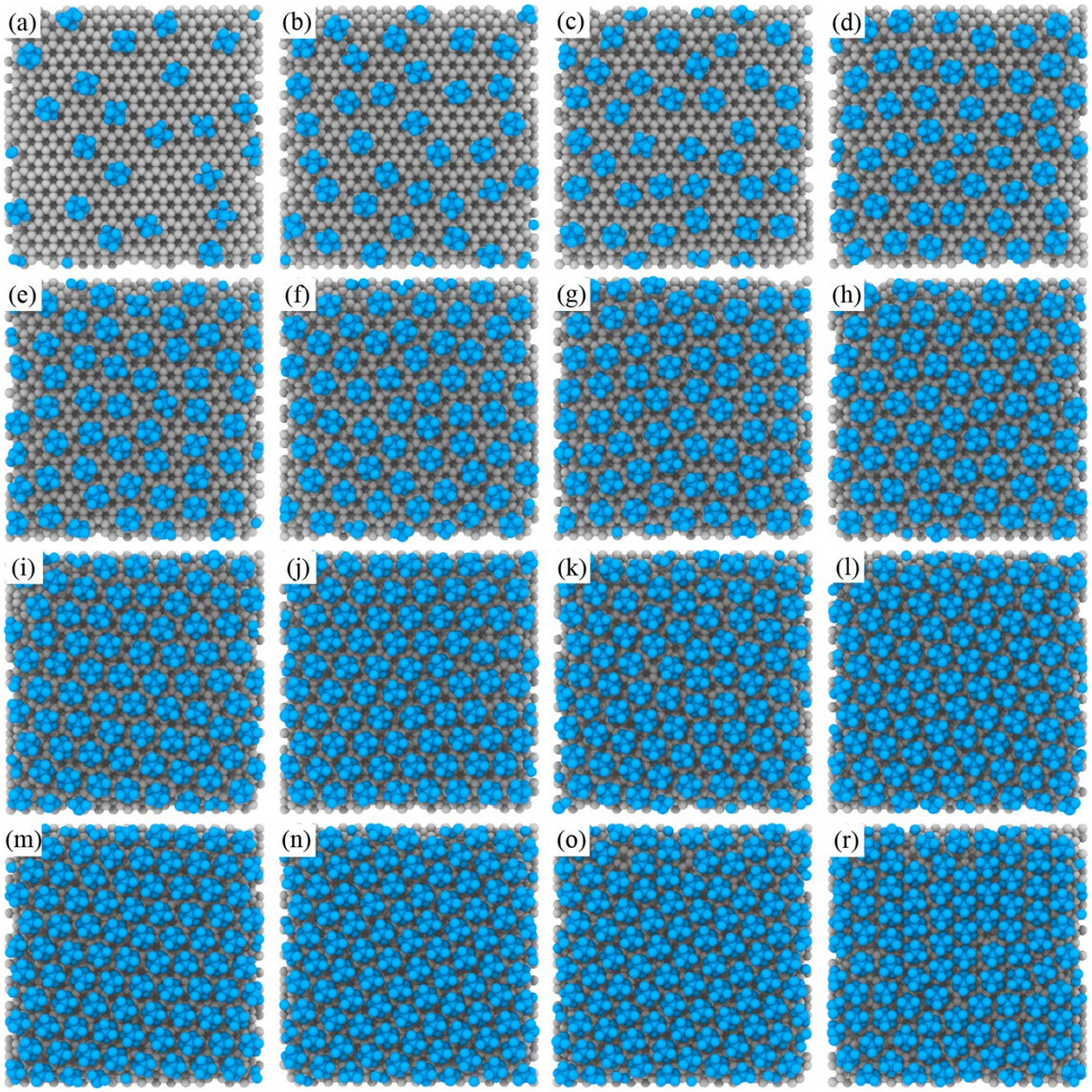

Figure S4. Atomic structure of PF_6^- on the first layer at the anode. The PF_6^- are colored in blue, while the anode is colored in light grey. The surface charge compensation parameter κ_{Anion} in (a)-(r) is 0.00, 0.13, 0.25, 0.38, 0.44, 0.50, 0.56, 0.63, 0.69, 0.75, 0.81, 0.88, 0.94, 1.00, 1.13 and 1.25, respectively. The $BMIM^+$ is not shown here for simplicity. A second counter ion layer appears when $\kappa_{Anion} > 1$. With the influence of this second counter ion layer, the ordering decreases in (o) and (r).

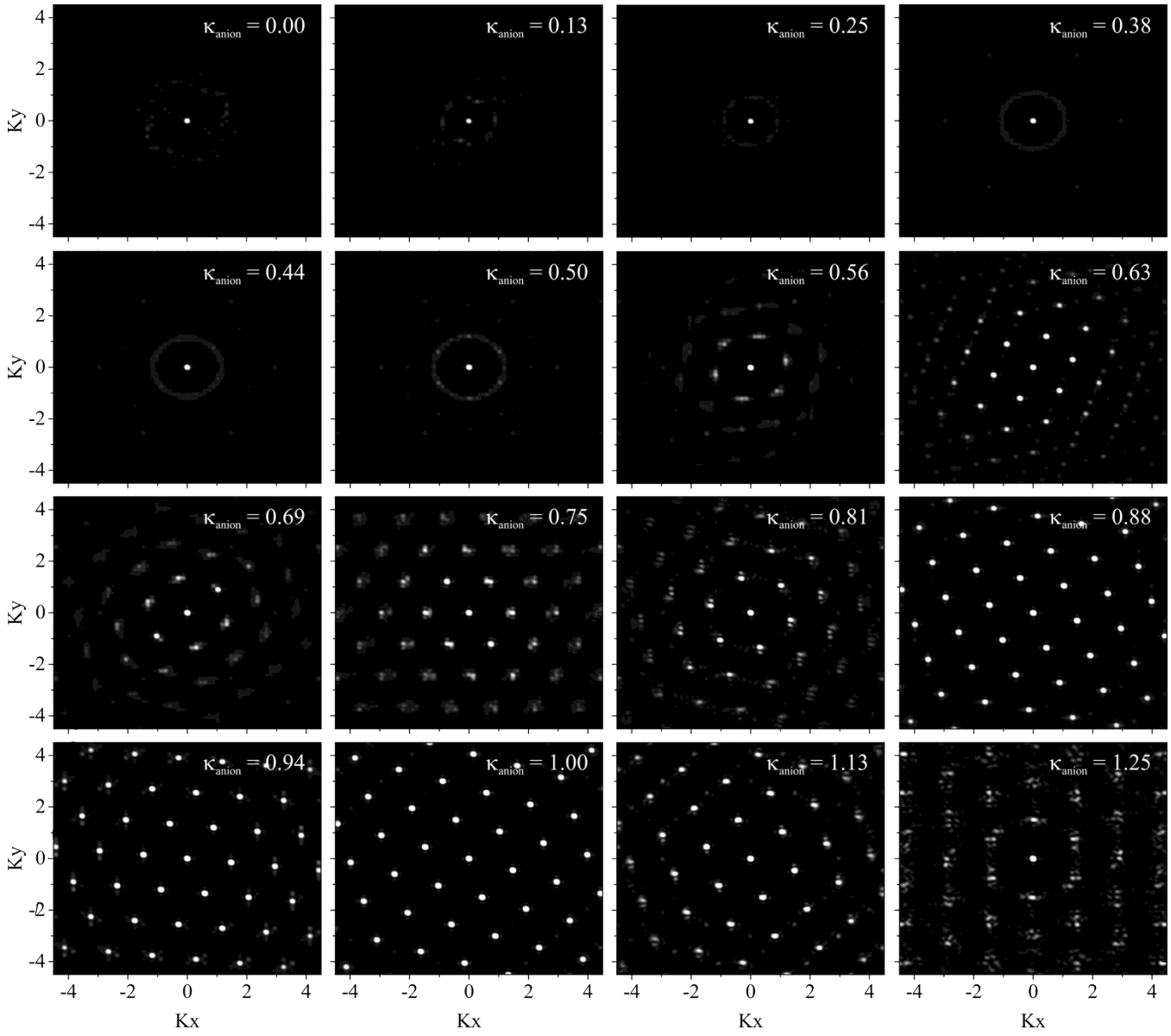

Figure S5. 2D structure factor S(k) profile of PF_6^- ions in the first layer at the anode. The surface charge compensation parameter κ_{Anion} here are the same as that in Figure S4.

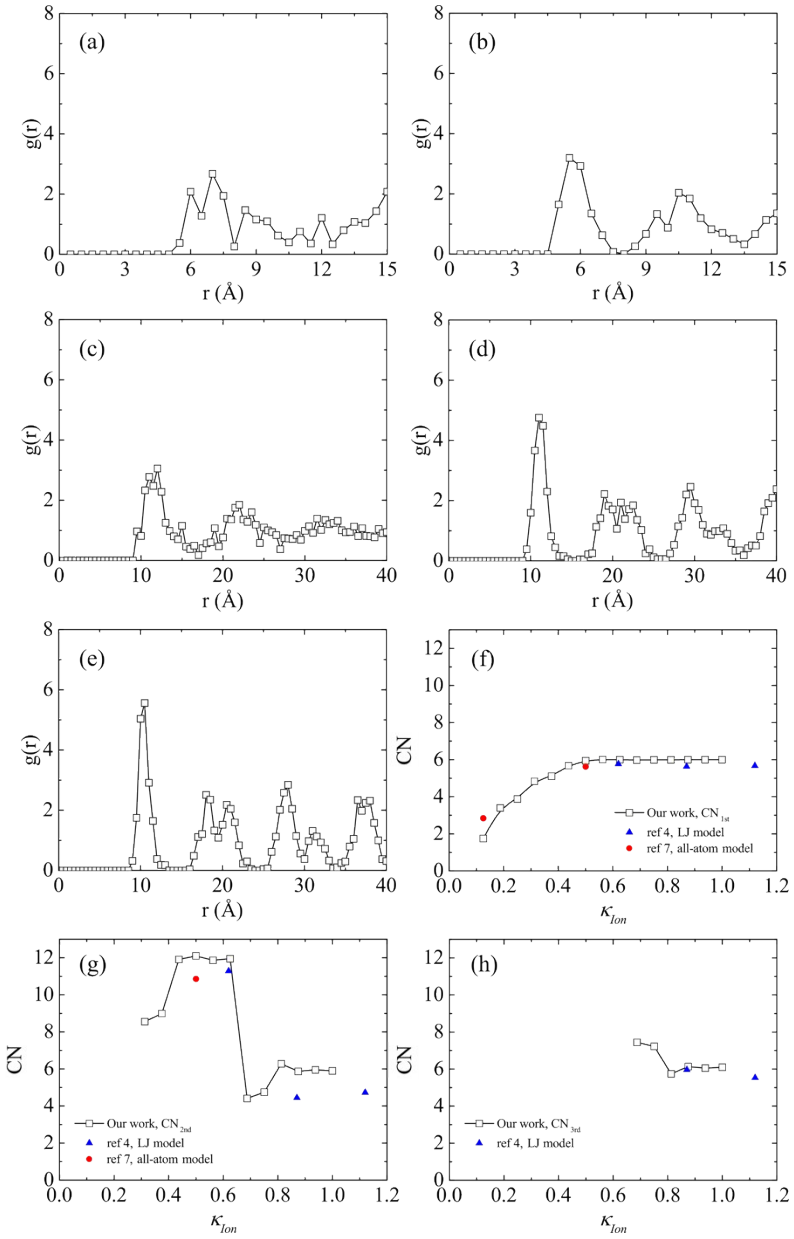

Figure S6. Coordination Number (CN) profiles of the simulation configurations in ref. 4and ref. 7. RDF profiles of first layer ion at σ = (a) 10, (b) 40 μC/cm^2 in ref. 7, and κ_{Anion} = (c) 0.62, (d) 0.87 and (e) 1.12 in ref. 4 are first calculated. Based on the results in (a)-(e), CN of first, second and third RDF peaks are calculated in (f), (g) and (h), respectively. CN calculated from ref. 4 is colored in blue and that from ref. 7 is colored in red. Surface charge density in ref. 7 was converted to κ_{Anion} and θ_{max} = 80 μC/cm^2.

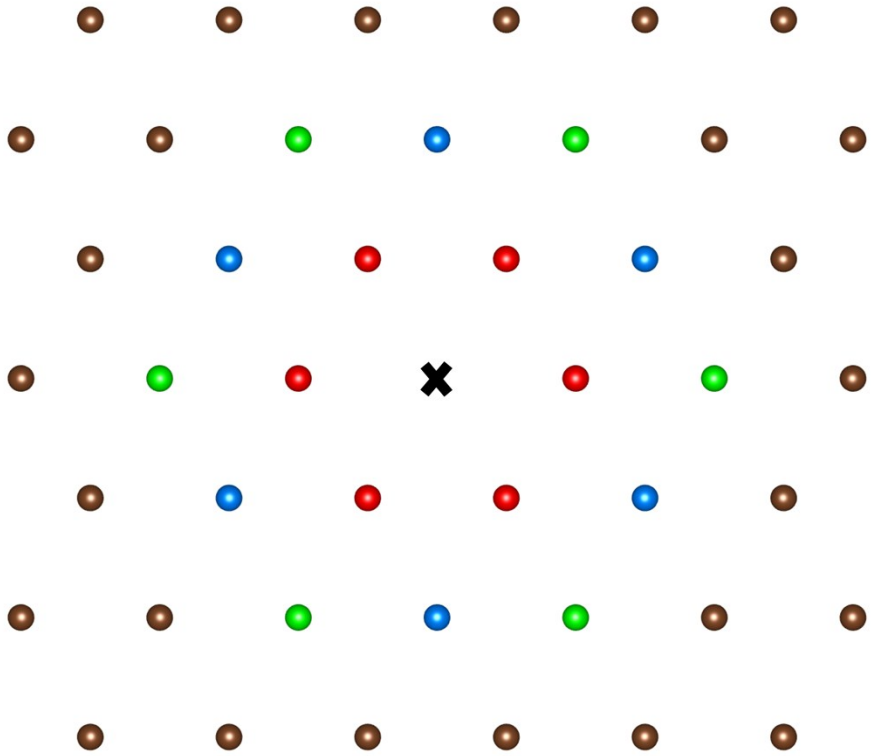

Figure S7. Neighboring atoms in hexagonal lattice. The first to third nearest neighbor atoms of the central black cross are colored in red, blue and green, respectively. Other atoms are colored in brown. The numbers of these neighbor atoms, i.e. CN_{1st}, CN_{2nd} and CN_{3rd}, are all 6.

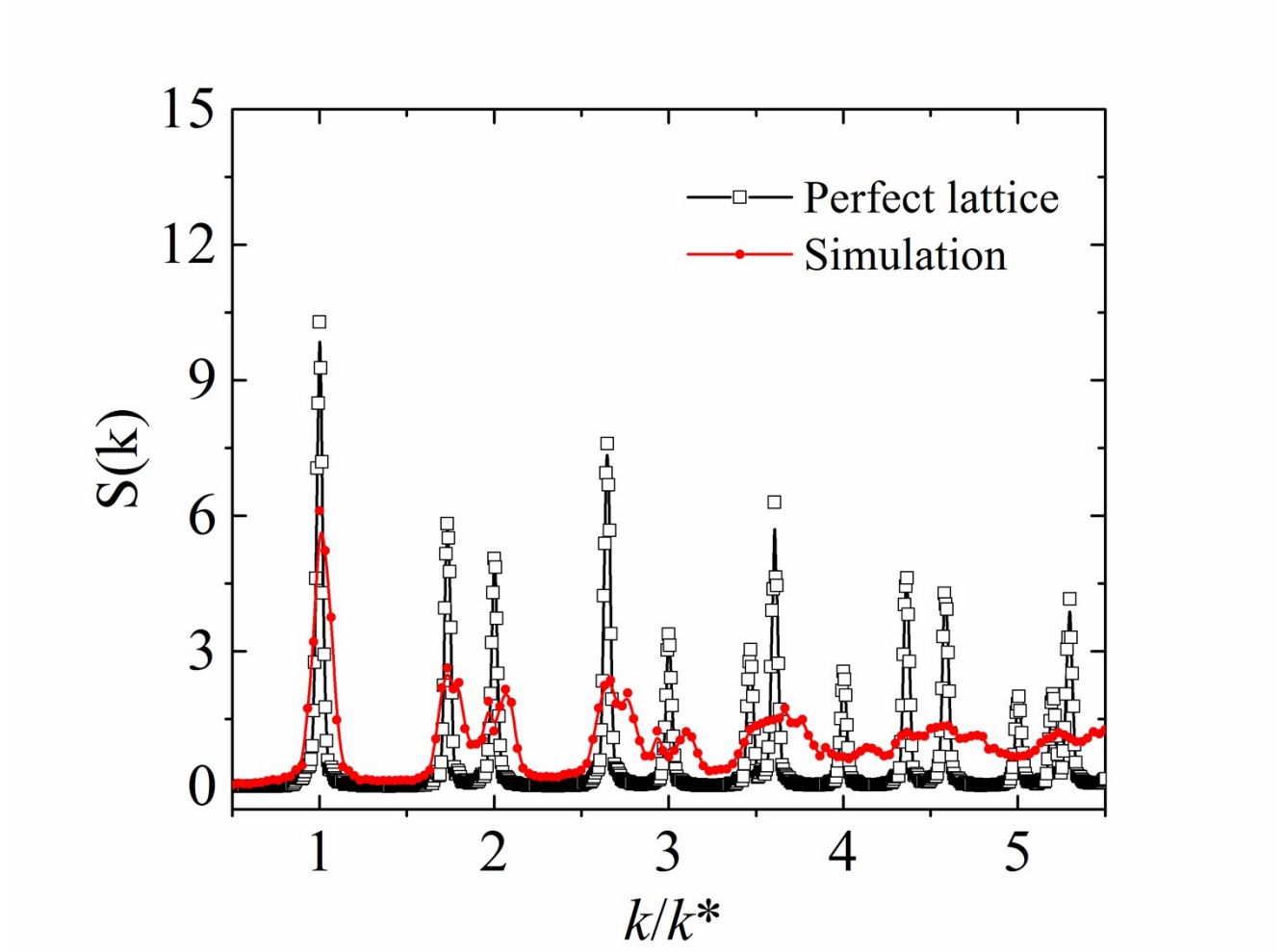

Figure S8. 2D S(k) profiles of perfect hexagonal lattice plane and first ion layer in the simulation. The S(k) profile of first ion layer in the simulation (red) was calculated at $\kappa_{\text{Anion}} = 1$. The S(k) profile of crystal plane (black) was calculated from 20 by 20 hexagonal supercell with 400 atoms. The k^* is the first peak position in each S(k) profile. Besides, the S(k) of hexagonal plane (black) was reduced to 1/30 of its original value to make two profiles comparable. It can be found that the first five red peaks match well with the hexagonal plane.

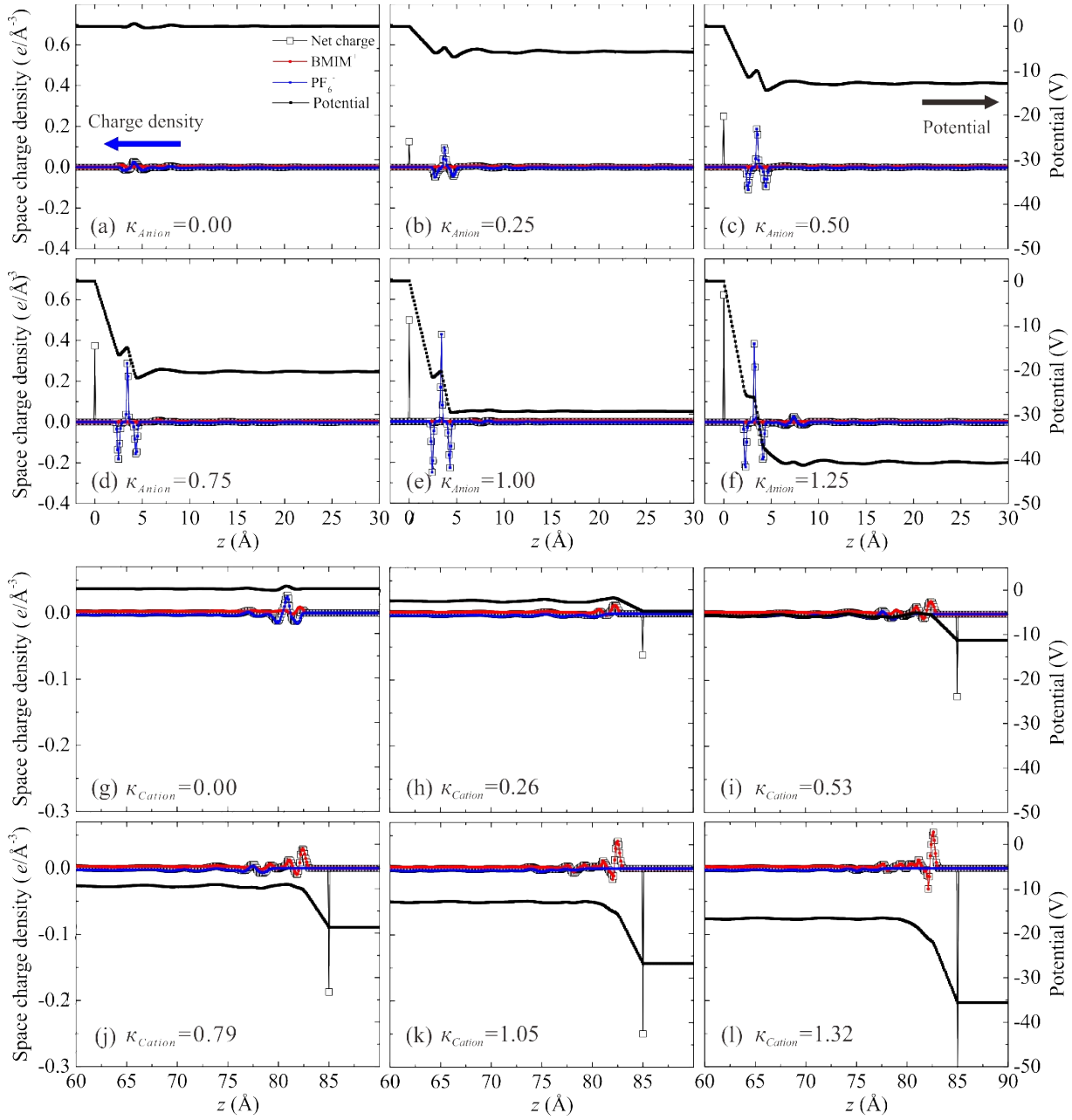

Figure S9. Charge density distribution and potential drop in *z* direction. The y axis of charge density profile is at left side and y axis of potential profile is at right side. The κ_{Anion} in (a)-(f) is 0.00, 0.25, 0.50, 0.75, 1.00 and 1.25, respectively. The κ_{Cation} in (g)-(l) is 0.00, 0.26, 0.53, 0.79, 1.05 and 1.32, respectively. The charge density of $BMIM^+$ and PF_6^- profiles are colored in red and blue, respectively. The net charge density and potential drop profiles are presented by black open and solid squares, respectively.

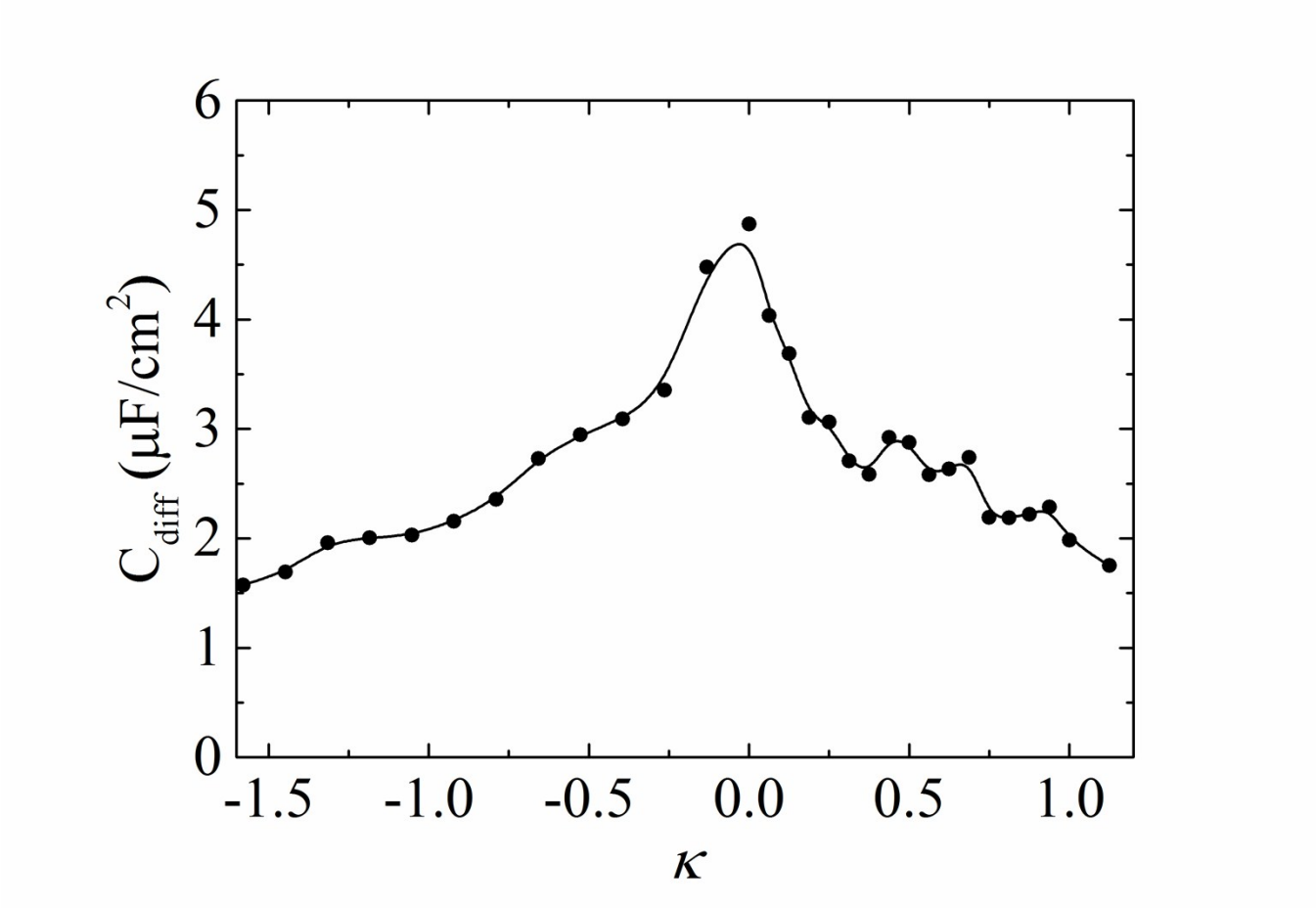

Figure S10. Bell shaped differential capacitance as a function of surface charge compensation parameter κ_{Anion}. The global maximum of differential capacitance is closed to the previous results of all atom MD simulation [7-10].

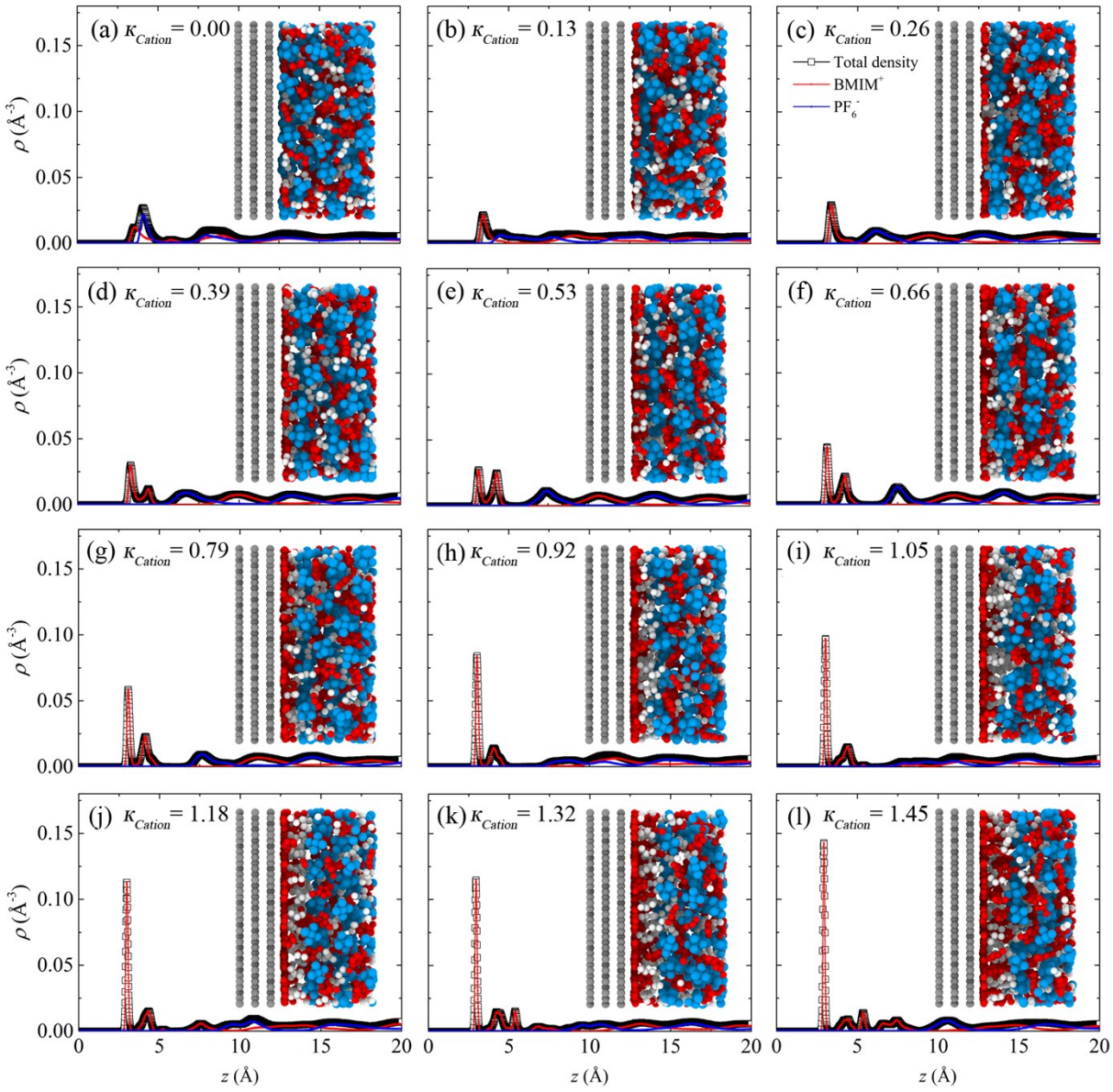

Figure S11. Number density distribution of ions in z direction near cathode. The surface charge compensation parameter κ_{Cation} in (a)-(l) is 0.00, 0.13, 0.26, 0.39, 0.53, 0.66, 0.79, 0.92, 1.05, 1.18, 1.32 and 1.45, respectively. The density profiles of $BMIM^+$, PF_6^- and the summation of both ions were colored in red, blue and black, respectively. The coordinates of $BMIM^+$ were determined by the center of mass of imidazole rings, since the side chains leave the surface after $\kappa_{Cation} > 0.5$. The surface of the cathode is located at z = 0 Å. The side views of ions near the anode were inserted.

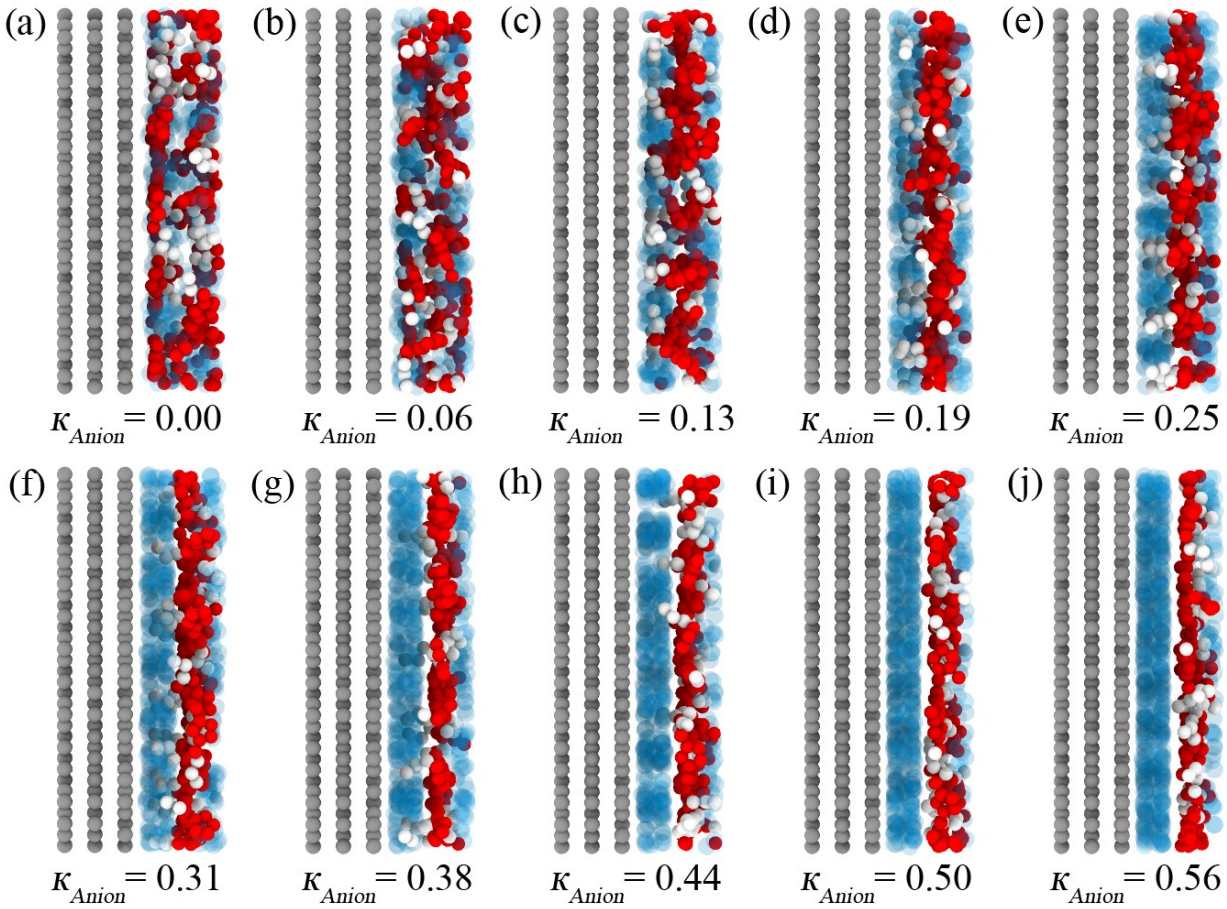

Figure S12. Side view of $BMIM^+$ near anode surface. $BMIM^+$ within 10 Å of the anode surface are shown. The surface charge compensation parameter κ_{Anion} in (a)-(j) is 0.00, 0.06, 0.13, 0.19, 0.25, 0.31, 0.38, 0.50, and 0.56, respectively. To show the red imidazole rings and white side chain clearly, blue PF_6^- are set to be semi-transparent. It can be found that the side chain (colored in white) of $BMIM^+$ leave the first PF_6^- layer at $\kappa_{Anion} = 0.5$.

3. Reference

1. J. N. Canongia Lopes, J. Deschamps and A. a H. Pádua, *J. Phys. Chem. B*, 2004, **108**, 2038–2047.
2. J. N. Canongia Lopes and A. A. H. Pádua, *J. Phys. Chem. B*, 2004, **108**, 16893–16898.
3. L. Martínez, R. Andrade, E. G. Birgin and J. M. Martínez, *J. Comput. Chem.*, 2009, **30**, 2157–2164.
4. K. Kirchner, T. Kirchner, V. Ivaništšev and M. V. Fedorov, *Electrochim. Acta*, 2013, **110**, 762–771.
5. V. Ivanistsev and M. V. Fedorov, *Electrochem. Soc. Interface*, 2014, **23**, 65–69.
6. V. Ivaništšev, S. O'Connor and M. V. Fedorov, *Electrochem. commun.*, 2014, **48**, 61–64.
7. E. Paek, a. J. Pak and G. S. Hwang, *J. Electrochem. Soc.*, 2012, **160**, A1–A10.
8. X. Si, S. Li, Y. Wang, S. Ye and T. Yan, *ChemPhysChem*, 2012, **13**, 1671–1676.
9. X. Liu, Y. Han and T. Yan, *ChemPhysChem*, 2014, **15**, 2503–2509.
10. Z. Hu, J. Vatamanu, O. Borodin and D. Bedrov, *Phys Chem Chem Phys*, 2013, **15**, 14234–14247.